

UNIVERSITY OF CALIFORNIA, SAN DIEGO

Understanding the Surface and Interface Properties of Electrode Materials
in Alkali-ion Batteries

--- A Combination of Experimental and Computational Studies

A dissertation submitted in partial satisfaction of the requirements for the degree

Doctor of Philosophy

in

Nanoengineering

by

Danna Qian

Committee in charge:

Ying Shirley Meng, Chair
Gaurav Arya
Renkun Chen
Miaofang Chi
Eric Fullerton
John Weare

2015

Copyright

Danna Qian, 2015

All rights reserved

The Dissertation of Danna Qian is approved, and it is acceptable in quality and form for publication on microfilm and electronically:

Chair

University of California, San Diego

2015

TABLE OF CONTENTS

SIGNATURE PAGE.....	iii
TABLE OF CONTENTS.....	iv
LIST OF FIGURES.....	vii
LIST OF TABLES.....	xii
ACKNOWLEDGEMENTS.....	xiii
VITA.....	xvi
ABSTRACT OF THE DISSERTATION.....	xviii
1 INTRODUCTION TO HIGH-ENERGY HIGH-POWER CATHODE MATERIAL FOR LITHIUM ION BATTERIES.....	1
1.1 Lithium Ion Batteries	1
1.2 High-energy high-power cathode materials in Li-ion batteries	3
1.3 Interface and surfaces.....	4
1.4 Objectives and overview.....	5
2 FIRST PRINCIPLES METHOD AND ITS APPLICATION ON ALKALI-ION BATTERY MATERIALS.....	8
2.1 Thermodynamics of intercalation materials.....	8
2.2 First principles energy calculations.....	9
2.2.1 General energy approximation.....	9
2.2.2 Density-functional theory.....	10
2.2.3 Generalized gradient approximation.....	10
2.2.4 Pseudopotential approximation.....	11
2.3 Surface and interface energy calculations.....	12
3 ADVANCED ANALYTICAL ELECTRON MICROSCOPY FOR ALKALI-ION BATTERIES.....	16
3.1 Introduction.....	16
3.2 Recent progress in TEM.....	17
3.3 High resolution electron microscopy for battery materials.....	19
3.3.1 Electrodes.....	19

3.3.2	Electrolyte.....	25
3.4	Dynamic/In-situ electron microscopy for battery research.....	28
3.4.1	Open-cell configuration.....	29
3.4.2	Liquid-cell configuration.....	31
3.4.3	All-solid-state micro-battery.....	32
3.5	Conclusions and perspectives.....	34
4	ELECTRON SPIN TRANSITION IN NANO-SIZE STOICHIOMETRIC LiCoO₂ AND ITS APPLICATIONS IN OXYGEN EVOLUTION REACTION / OXYGEN REDUCTION REACTION (OER/ORR) CATALYTIC PROCESS.....	42
4.1	Electron spin transition in nano-size stoichiometric LCO.....	42
4.1.1	Introduction.....	42
4.1.2	Methodologies.....	43
4.1.2.1	Computation.....	43
4.1.2.2	Synthesis.....	44
4.1.2.3	XRD.....	45
4.1.2.4	XPS.....	45
4.1.2.5	⁷ Li NMR.....	45
4.1.2.6	Fitting Equation for the Curie Constant.....	46
4.1.3	Results and Discussions.....	46
4.1.4	Conclusions.....	52
4.2	The application of surface-spin-transitioned nano-size stoichiometric LCO in OER/ORR catalytic process.....	53
4.2.1	Introduction.....	53
4.2.2	Methodologies.....	54
4.2.2.1	Electrochemical measurements.....	54
4.2.2.2	TEM.....	54
4.2.2.3	EELS.....	55
4.2.3	Results and Discussions.....	55
4.2.4	Conclusions.....	58
5	UNCOVERING THE ROLES OF OXYGEN VACANCY ON CATION MIGRATION IN LITHIUM EXCESS LAYERED OXIDES.....	77
5.1	Introduction.....	77
5.2	Methodologies.....	78
5.2.1	STEM/EELS.....	78
5.2.2	Computation.....	79
5.3	Results and Discussions.....	80
5.4	Conclusions.....	85

6	SURFACE COATING ON CATHODE MATERIALS IN LIB.....	91
6.1	Lithium lanthanum titanium oxides: a fast ionic conductive coating for lithium-ion battery cathodes.....	91
6.1.1	Introduction.....	91
6.1.2	Methodologies.....	93
6.1.2.1	Computational methods.....	93
6.1.2.2	Experimental methods.....	94
6.1.2.3	Electrochemical characterization.....	95
6.1.3	Results.....	96
6.1.3.1	Computational results.....	96
6.1.3.2	Experimental results.....	98
6.1.4	Discussions.....	103
6.1.5	Conclusions.....	106
6.2	AlF ₃ coating for lithium-ion battery cathodes.....	106
6.2.1	Introduction.....	106
6.2.2	Methodologies.....	108
6.2.2.1	TEM.....	108
6.2.2.2	a-STEM/EELS.....	108
6.2.3	Results and Discussions.....	109
6.2.4	Conclusions.....	111
7	STEM/EELS STUDY OF P2-Na_{2/3}[Fe_{1/3}Mn_{2/3}]O₂.....	122
7.1	Introduction.....	122
7.2	Methodologies.....	123
7.3	Results and Discussions.....	124
7.4	Conclusions.....	125
8	SUMMARY AND FUTURE WORK.....	130
8.1	Summary.....	130
8.2	Future work.....	131
8.2.1	Surface and interface properties of Na based electrode materials....	131
8.2.2	Computational study on layer/spinel and layer/rocksalt interface....	132
	REFERENCES.....	133

LIST OF FIGURES

Figure 1.1: Working principles of LIB (charging)	6
Figure 1.2: Theoretical and practical gravimetric energy densities of different cathode materials.....	6
Figure 1.3: Crystal structure of layered LiMO_2 (Blue: transition metal ions; Red: Li ions)	7
Figure 2.1: Three types of Tasker ionic crystal surfaces.....	15
Figure 2.2: Schematic plot of surface and bulk.....	15
Figure 3.1: Overview of the implementation of TEM in AIB.....	36
Figure 3.2: HAADF STEM images of Li-excess materials (a) pristine and (b) after cycling; (c) &(d) EELS comparison of pristine and cycled surface and bulk; (e) Spatial resolved O K-edge EELS from surface to bulk in cycled Li-excess.....	37
Figure 3.3: (a) Top: Schematic figure of the probable configuration of Fe_{Li} with a higher Fe oxidation state. Bottom: (Left) EELS data of Fe_{Li} and the Fe in bulk. (Right) Compared L3/L2 ratio with reference different iron compounds; (b) ABF image of half charged state showing the Li staging.....	38
Figure 3.4: (a) HAADF and (b) ABF of local clustering of A-site vacancies and O4 square window lithium. (c) HAADF STEM images of a LLTO grain boundary. EELS data of (d) Li K edge, (e) Ti L edge for the grain boundary and the bulk.....	39
Figure 3.5: (a) Schematic of the volatile cell set up; (b) a high density of dislocations emerging from the reaction front was revealed in single SnO_2 nanowire.....	40
Figure 3.6: (a) Experimental set up of non-volatile cell set up with liquid electrolyte; (b) & (c) in-situ observation of inhomogeneous lithiation, lithium metal dendritic growth and solid-electrolyte interface formation; (d) an example of all-solid-state battery.....	41

Figure 4.1: (a) {104} and (b) {110} surfaces of LiCoO ₂ (c) Octahedrally, square pyramid and pseudo-tetrahedrally coordinated Co ions. (red- oxygen, green – lithium, blue Co).....	60
Figure 4.2: Spin density plot of the {104} plane of the bulk (a) and the surface (b). (Notice the scale differences in the spin density).....	60
Figure 4.3: (a) XRD and (b) XPS spectra of nano-sized stoichiometric LiCoO ₂	61
Figure 4.4: ⁷ Li MAS NMR spectra of LiCoO ₂ with varying particle sizes. (a) Percentages of the Li near by low spin Co (III) in LiCoO ₂ are listed in (a). Peak assignment and percentages of Li ions in environments nearby paramagnetic ions can be found in enlarged spectra. (b) Asterisks	62
Figure 4.5: (a) Molar magnetic susceptibilities of particle size 10nm, 16nm, 20nm, 30nm and 40nm samples as a function of temperature. (b) The Curie constants of these samples determined from the 1/χ vs T. (Both are measured with sample holder corrected).....	62
Figure 4.6: Projected density of states (DOS) of Co ions on the surface and bulk of LiCoO ₂ . Upper: {104} surface Co with IS (left) and bulk Co with LS (right); Bottom: {110} Surface Co with IS (left) and Bulk Co with LS (right).....	63
Figure 4.7: Electrochemical data for both bulk-LiCoO ₂ (black) and 10nm-LiCoO ₂ (red) in a lithium half-cell.....	64
Figure 4.8: (a) Representative TEM image of a nanorod from the LiCoO ₂ sample with an average rod diameter of 40 nm. (b) High-resolution TEM image of a representative nanorod LiCoO ₂ with its associated selected-area electron diffraction pattern. (c) Histograms of the length and diameter distributions...65	65
Figure 4.9: (a)(b) Representative EELS spectra of pristine 9-nm LiCoO ₂ : (a) Co L edge, (b) O K edge. (c)-(e) Two types of representative EELS spectra of 9-nm sample held at 0.7 V vs. RHE for ORR. Middle row is one set of (c) Co L edge and (d) O K edge (case 1); bottom row (e) and (f) is the other set.....	66

Figure 4.10: (a) Cyclic voltammetry of ORR current of different LiCoO ₂ samples in O ₂ -saturated 0.1 M KOH at 10 mV/s. (b) Potentiostatic measurements of OER current of different LiCoO ₂ samples in O ₂ -saturated 0.1 M KOH at different voltages. (c-f) Tafel plots of ORR and OER activities.....	67
Figure 4.11: (a) CV curves of different Co compounds in the Co redox region. (b) Calculation scheme of charge transfer during Co 2 ^{+/3+} and 3 ^{+/4+} redox reactions by integrating the redox peaks. (c) Charge transferred per surface area of tip and side surfaces of LiCoO ₂ during 2 ^{+/3+} and 3 ^{+/4+} redox.....	68
Figure 4.12. Two types of representative EELS spectra of 9 nm sample held at 1.55 V vs. RHE for OER. Upper row is one set of (a) Co L edge and (b) O K edge (case 1); bottom row (c) and (d) is the other set of spectra (case 2).....	69
Figure 4.13. Representative EELS spectra of 9 nm sample that was immersed in 0.1 M KOH electrolyte for 1 hour without applying any potential. Then sample was rinsed by DI water and tried in air at room temperature. These spectra were taken under 300 kV. (a) Co L edge and (b) O K edge.....	69
Figure 5.1: Spatial resolved O K-edge EELS spectra from bulk to surface.....	87
Figure 5.2: (a) Atomic configurations of Li[Li _{1/6} Ni _{1/4} Mn _{7/12}]O ₂ ; (b) Oxygen vacancy formation energy vs. Li concentration.....	88
Figure 5.3: Ni diffusion barriers with oxygen vacancies in different positions at Li _{15/28} Ni _{1/4} Mn _{7/12} O ₂	89
Figure 5.4: Calculated Ni diffusion barriers with oxygen vacancies in different positions at Li _{20/28} Ni _{1/4} Mn _{7/12} O ₂	89
Figure 5.5: Neighboring TM valence change after introduction of oxygen vacancy at Li _{20/28} Ni _{1/4} Mn _{7/12} O ₂	90
Figure 5.6: Mn diffusion barriers with oxygen vacancies in different positions at Li _{20/28} Ni _{1/4} Mn _{7/12} O ₂	90
Figure 6.1: Computational model structure of Li _{0.125} La _{0.625} TiO ₃ (a) and Li _{0.35} La _{0.55} TiO ₃ (d). Planes of interest used in NEB calculation of low lithium concentration	

	(b) and high lithium concentration (e). (c) and (f) are the after relaxation structure of planes in (b) and (e) respectively.....	112
Figure 6.2:	(a) $x=3/4$ plane of low lithium concentration with all equilibrium states and middle images. Two crosses are the images between Li1 and Li2, Li2 and Li3 respectively. (Other images can get from symmetry). (b) (c) Illustration of vertical oxygen square window.....	113
Figure 6.3:	Estimated Li diffusion path in La-poor layer (green dash lines) in low lithium concentration scenario (a) and high lithium concentration scenario (b).....	114
Figure 6.4:	Structural characterization of pristine and LLTO coated samples. (a) (b) and (c)(d) are the SEM images of pristine and LLT5, respectively; (e) (f) and (g) are EDS results of pristine, LLT1 and LLT5, respectively. The inset in (c) and (d) is the TEM image of LLT5.....	115
Figure 6.5:	(a) XRD results of pristine, LLT1, LLT2, and LLT5. (b) Zoom in of $23^\circ \sim 26.5^\circ$. (c) Zoom in of $30.5^\circ \sim 34.5^\circ$	116
Figure 6.6:	Electrochemical cycling and rate capability of pristine and coated electrodes. (a) Cycling retention properties of pristine, LLT1, LLT2 and LLT5. Rate capability of pristine (b) and LLT1 (c).....	117
Figure 6.7:	(a) Calculated Li ion diffusion coefficient of pristine (black) and LLT1 (red) from PITT tests. Impedance spectra (100kHz – 100mHz) of pristine (b) and LLT1 (c) obtained from the cell at 4.2V. Dashed lines are the CNLS fittings of the impedance spectra of the equivalent circuit model.....	117
Figure 6.8:	EELS mapping of LLT5 (a) before and (b) after cycling. Green: Li; Blue: La; Red: Ti.....	118
Figure 6.9:	The TEM and STEM of LNMO and NALNMO, a) TEM of LNMO, b) and c) TEM of NALNMO, d) STEM of NALNMO.....	119
Figure 6.10:	High-resolution S/TEM images of the bulk and surface of NALNMO.....	120
Figure 6.11:	The STEM of NALNMO with step scan of Mn EELS L edge and O EELS K edge.....	120
Figure 7.1:	HAADF and ABF images of pristine $P2-Na_{2/3}[Fe_{1/3}Mn_{2/3}]O_2$	127

Figure 7.2: [001] zone axis ED of pristine, charged and discharged sample.....	127
Figure 7.3: EELS spectra comparison of pristine, charged and discharged sample.....	128
Figure 7.4: Mechanism figure.....	128

LIST OF TABLES

Table 4.1: Synthesis conditions and altered parameters to give the desired stoichiometric LiCoO ₂ particle size.	70
Table 4.2: Rietveld Refinement fit parameters and the calculated <i>a</i> and <i>c</i> lattice parameters for the various sized stoichiometric LiCoO ₂ nanoparticles.....	71
Table 4.3: Calculated surface energy w/o spin transition compared with literature.....	72
Table 4.4: The mass-normalized tip, side and total surface areas of each LiCoO ₂ sample, computed using the particle size distributions collected from TEM images.....	73
Table 4.5: The O K pre-peak area of tips and sides.....	74
Table 4.6: The mass-normalized and total-surface normalized charge transfer during Co 2+/3+ and 3+/4+ redox processes of each LiCoO ₂ sample.....	75
Table 4.7: The Co L3/L2 ratios of tips and sides.....	76
Table 6.1: List of the layer sequence of three models and energy values obtained after relaxation.....	121
Table 7.1: EELS quantification of Fe and Mn oxidation states for pristine, charged and discharged samples.....	129

ACKNOWLEDGEMENTS

First of all, I would like to thank my thesis advisor Dr. Ying Shirley Meng for providing me all the opportunities to do this research and her continuous support, and good advice throughout the projects. I was sincerely honored to meet and work with her. I shall never forget her endless advice and help. I would also like to thank my other advisor during my ORNL stay, Dr. Miaofang Chi for her support and advice. I would like to express the deepest gratitude to my other committee members: Dr. Gaurav Arya, Dr. Renkun Chen, Dr. Eric Fullerton, Dr. John Weare for their time and guidance.

Secondly, I would like to acknowledge my collaborators and co-authors in UCSD, Dr. Bo Xu, Dr. Kyler Carroll, Dr. Christopher R. Fell, Dr. Dhamadaran Santhanegopalan Hyung-man Cho and Haodong Liu in LESC group as well as all other collaboration works. I am also grateful to all the group mates in LESC who have helped and inspired me in many ways.

Finally, I would like to express my thanks to my collaborators and co-authors outside LESC, Alex Han, Dr. Marcel Risch and Dr. Yang Shao-Horn from MIT, Dr. Clare P. Grey at University of Cambridge, Dr. Hailong Chen from Georgia Tech, Dr. Cheng Ma and Dr. Karen More from Oak Ridge National Laboratory for their invaluable help throughout the projects.

Chapter 1, in part, is a reprint of the material “Recent progress in cathode materials research for advanced lithium ion batteries”, as it appears in *Materials Science and Engineering R*, 73(5-6), 51-65, by Bo Xu, Danna Qian, Ziyang Wang, Ying Shirley Meng, 2012. The dissertation author was the co-primary investigator and author of the paper.

Chapter 3, in full, is a reprint of the material “Advanced analytical electron microscopy for alkali-ion batteries”, as currently prepared for publication. The dissertation author was the primary investigator and author of this paper. Most of the writing was conducted by the author.

Chapter 4, part 1, in full, is reprinted with permission from the following paper “Electronic spin transition in nanosize stoichiometric lithium cobalt oxide”, Journal of the American Chemical Society, 2012, 134(14), 6096-6099 by Danna Qian, Y. Hinuma, H. Chen, L-S Du, K. Carroll, G. Ceder, C. P. Grey, Y. S. Meng, Copyright (2012) American Chemical Society. The second part, in part, is reprint from “The role of LiCoO₂ surface termination in oxygen reduction and evolution kinetics” being submitted by B. Han, Danna Qian (equally contributed), M. Risch, H. Chen, M. Chi, Y. S. Meng, Y. S-H.. The dissertation author was the primary investigator and author of the papers.

Chapter 5, in full, is a reprint of the material “Uncovering the roles of oxygen vacancies in cation migration in lithium excess layered oxides”, Phys. Chem. Chem. Phys., 2014, 16, 14665, reproduced by permission of the PCCP Owner Societies. The dissertation author was the primary investigator and author of the paper.

Chapter 6, Part 1, in full, is a reprint with the permission of the material “Lithium lanthanum titanium oxides: a fast ionic conductive coating for lithium-ion battery cathodes”, Chemistry of Materials, 2012, 24(14), 2744, by Danna Qian, B. Xu, H. -M. Cho, T. Hatsukade, K. J. Carroll, Y. S. Meng, Copyright (2012) American Chemical Society. The dissertation author is the primary investigator and author of the material. Part2, in part, is a reprint of the material “Understanding the role of NH₄⁺ and Al₂O₃

surface co-modification on lithium-excess layered oxide $\text{Li}_{1.2}\text{Ni}_{0.2}\text{Mn}_{0.6}\text{O}_2$ ” prepared for publication. The dissertation author is the primary investigator and author.

Chapter 7, in full, is a reprint of the material “STEM/EELS study of $\text{P2-Na}_{2/3}[\text{Fe}_{1/3}\text{Mn}_{2/3}]\text{O}_2$ ”, which is in preparation for submission. The dissertation author is the primary investigator and author.

I would like to acknowledge the financial support from Northeastern Center for Chemical Energy Storage (NECCES), an Energy Frontier Research Center funded by the U. S. Department of Energy, and Advanced Short-Term Research Opportunity (ASTRO) program in ORNL. I would like to acknowledge Texas Advanced Computer Center for providing computation resources.

For the last but not least, my deepest gratitude to my parents, Xiaoman Qian and Xiaochun Yu, my husband, Ying Chen and the baby we are expecting. Their love, patience and unselfish support make everything possible.

VITA

2009 B. S. in Chemistry University of Science and Technology of China
2015 Ph. D. in Nanoengineering University of California, San Diego, USA

PUBLICATIONS

1. **Danna Qian**, B. Xu, H-M Cho, T. Hatsukade, K. Carroll, Y. S. Meng*, “Performance Improvement in Lithium Lanthanum Titanate Coated $\text{LiNi}_{0.8}\text{Co}_{0.15}\text{Al}_{0.05}\text{O}_2$ --- A combination of first-principles calculations and experimental studies”, *Chemistry of Materials*, 2012, 24(14), 2744-2751
2. **Danna Qian**, Y. Hinuma, H. Chen, L-S Du, K. Carroll, G. Ceder, C. P. Grey, Y. S. Meng*, “Electronic spin transition in nanosize stoichiometric lithium cobalt oxide”, *Journal of the American Chemical Society*, 2012, 134(14), 6096-6099
3. B. Xu, **Danna Qian**, Z. Wang, Y. S. Meng*, “Recent Progress in Cathode Materials Research for Advanced Lithium Ion Batteries”, *Materials Science and Engineering R*, 2012, 73(5-6), 51-65
4. K. Carroll, **Danna Qian**, C. Fell, S. Calvin, G. M. Veith, M. Chi, L. Baggetto, Y. S. Meng*, “Probing the electrode/electrolyte interface in the Li-excess material $\text{Li}_{1.2}\text{Ni}_{0.2}\text{Mn}_{0.6}\text{O}_2$ ”, *Phys. Chem. Chem. Phys.*, 2013, 15, 11128
5. C. Fell, **Danna Qian**, K. Carroll, M. Chi, J. L. Jones, Y. S. Meng*, “Correlation between oxygen vacancy, microstrain and cation distribution in Lithium-excess layered oxides during the first electrochemical cycle”, *Chem. Mater.*, 2013, 25(9), 1621-1629
6. Y. Janssen, D. Santhanagopalan, **Danna Qian**, M. Chi, X. Wang, C. Hoffman, Y. S. Meng and P. Khalifah*, “Reciprocal Salt Flux Growth of LiFePO_4 single crystals with Controlled Defect Concentrations”, *Chem. Mater.*, 2013, 25(22), 4574
7. D. Santhanagopalan, **Danna Qian**, T. Mcgilvary, Z. Wang, F. Wang, F. Camino, J. Graetz, N. Dudney, Y. S. Meng*, “Interface limited lithium transport in all-solid-state nano-batteries”, *J. Phys. Chem. Lett.*, 2014, 5, 298
8. **Danna Qian**, N. Hagh, Y. S. Meng*, “Insight into designing high-energy high-power cathode material for lithium ion batteries”, *ECS Electrochemistry Letters*, 2014, 3(7), A72
9. **Danna Qian**, B. Xu, M. Chi, Y. S. Meng*, “Uncovering the roles of oxygen vacancy on cation migration in lithium excess layered oxides”, *Phys. Chem. Chem. Phys.*, 2014, 16, 14665
10. **Danna Qian**, C. Ma, K. More, Y. S. Meng, M. Chi*, “Advanced analytical electron microscopy for alkaline ion batteries”, In preparation
11. Y.-S. Yu, C. Kim, D. Shapiro, M. Farmand, **Danna Qian**, T. Tyliczszak, D. Kilcoyne, S. Marchesini, J. Joseh, P. Denes, T. Warwick, F. Strobridge, C. P. Grey, H. Padmore, Y. S. Meng, R. Kosteci, J. Cabana*, “Effect of crystal size on the nanoscale chemical phase distribution and fracture in Li_xFePO_4 ”, Submitted.
12. **(Equal contribution)** B. Han†, **Danna Qian**†, M. Risch, H. Chen, M. Chi, Y. S. Meng*, Yang Shao-Horn*, “The Role of LiCoO_2 Surface Termination in Oxygen Reduction and Evolution Kinetics”, Submitted.

13. H. Liu, **Danna Qian**, M. Zhang, K. Carroll, L. Baggetto, K. An, M. Chi, Y. Chen, D. Lau, G. Veith, Y. S. Meng*, “Understanding the role of NH_4^+ and Al_2O_3 surface co-modification on lithium-excess layered oxide $\text{Li}_{1.2}\text{Ni}_{0.2}\text{Mn}_{0.6}\text{O}_2$ ”, In preparation
14. Q. Bao, M. Zhang, L. Wu, Y. Xia, J. Wang, **Danna Qian**, H. Liu, Y. S. Meng*, Y. Zhu, Z. Liu*, “Gas-solid interface reactivation of lithium-rich layered cathode with high capacity and improved rate capability for lithium-ion battery”, In preparation.
15. H. Liu, Y. Chen, K. An, S. Venkatachalam, **Danna Qian**, M. Zhang, Y. S. Meng*, “Probing the actives of Li and O in advanced Li-ion batteries via *In-operando* neutron diffraction”, In preparation.
16. **D. Qian**, C. Ma, J. Xu, K. More, Y. S. Meng, M. Chi*, “STEM/EELS study of $\text{P2-Na}_{2/3}[\text{Fe}_{1/3}\text{Mn}_{2/3}]\text{O}_2$ ”, In preparation.

ABSTRACT OF THE DISSERTATION

Understanding the Surface and Interface Properties of Electrode Materials

in Alkali-ion Batteries

--- A Combination of Experimental and Computational Studies

by

Danna Qian

Doctor of Philosophy in NanoEngineering

University of California, San Diego, 2015

Professor Ying Shirley Meng, Chair

In order to realize the commercialization of alkali-ion batteries (AIB) in electric vehicles and smart grid systems, further improvements are demanded in multiple aspects, especially the energy/power density, safety and cycle life. Due to the complexity of the system, besides each separate component, surface and interface are critical in understanding and optimizing the system.

In this dissertation, systematic studies are performed on the nanosizing effect, the surface phase transformation and surface coating of Li-intercalation cathode materials by a combination of first principles and experimental studies. In the first part, the surface spin transition of LiCoO_2 (LCO) was found based on first principles calculations. Different sizes of LCO were synthesized and the spin transition on the surface was

confirmed by other characterization techniques. The OER/ORR activities profoundly increased at the spin-transitioned surfaces. The study shed lights on the electronic properties tuning in nanosizing process, which would affect functional properties.

In the second part, the structural and chemical evolutions during electrochemical process of the Li-excess compound was probed by a combination of high-end characterization techniques especially STEM/EELS. A second phase generation together with oxygen vacancy formation and microstrain formation was found at the first cycle plateau region. A novel oxygen vacancy assisted transition metal migration mechanism was proposed using first principles calculations. These findings lead to an increased understanding of the performance fading mechanism of Li-excess family compounds, providing new insights in optimization their rate performances.

In the third part, the surface coating of LLTO has been investigated for an improved electrochemical performance of the NCA combining computation with other electrochemical tests. The good ionic conductor LLTO increases the system's ion conductivity thus the electrochemical performance. Similar investigations have also been carried out in AlF_3 coatings. These studies help the understanding of coating effect of electrode materials.

In the fourth part, a detailed STEM/EELS study on the P2 type Na cathode material was carried out.

1 INTRODUCTION TO HIGH-ENERGY HIGH-POWER CATHODE MATERIAL FOR LITHIUM ION BATTERIES

Lithium ion batteries (LIB), regarded as one of the near-term solutions for green energy storage, are well developed for portable electronic devices and have been widely used in the past twenty years. Recently, with the emerge of hybrid electric vehicles (HEV) and electric vehicles (EV) such as Toyota Prius, Nissan Leaf, Tesla etc., increasing effort has been focused on improving the energy/power density, cycling life and safety issues of the system. Further development on LIB system and materials is thus necessary and urgent.

1.1 Lithium ion batteries

A lithium ion battery can work as the energy storage device by converting electric energy into electrochemical energy. The basic working principles of LIB are shown in Figure 1.1. There are three key components in a LIB system: cathode, anode and electrolyte. For today's commercialized LIB system, both cathode and anode materials are intercalation materials. The transition metal oxides in cathode (graphite in anode) consist of a largely unchangeable host with specific sites for Li ions to be intercalated in. All Li ions are in the cathode sides initially and the battery system is assembled in "discharged" status. While charging, Li ions are extracted from the cathode host, solvate into and move through the non-aqueous electrolyte, and intercalate into the anode host. Meanwhile, electrons also move from cathode to anode through the outside current collectors forming an electric circuit. The chemical potential of Li is much higher in the anode than in the cathode, thus the electric energy is stored in the form of

(electro)chemical energy. Such process is reversed when the battery is discharging where the electrochemical energy is released in the form of electric energy. The cathode region and anode region are separated by the separator, a micro-porous membrane that allows the electrolyte to penetrate and prevent shorting between the two electrodes. The electrolyte should be ionically conducting and electronically insulating in principle, however the actual properties of the electrolyte is much more complicated. During the first cycle, a so-called solid-electrolyte-interphase (SEI) layer will be formed on the surface of electrodes due to the decomposition of organic electrolyte at extreme voltage range (typically $<1.2\text{V}$ or $>4.6\text{V}$). In current LIB technology, the cell voltage and capacities are mainly determined by the cathode material that is also the limiting factor for Li transportation rate. The developments of cathode materials therefore become extremely crucial and receive much attention in recent decade.

Since 1980 when the LiCoO_2 was demonstrated firstly as a possible cathode material for rechargeable lithium battery, the transition metal intercalation oxides have caught the major research interests as the LIB cathodes. Categorized by structure, the conventional cathode materials include layered compounds LiMO_2 ($\text{M} = \text{Co}, \text{Ni}, \text{Mn}$ etc.), spinel compounds LiM_2O_4 ($\text{M} = \text{Mn}$ etc.), and olivine compounds LiMPO_4 ($\text{M} = \text{Fe}, \text{Mn}, \text{Ni}, \text{Co}$ etc.). Most of the researches are performed on these materials and their derivatives. New structure intercalation materials such as silicates, borates and tavorite are also gaining increasing attentions in recent years. During the materials optimization and development, following designing criterions are often considered: 1) Energy density; 2) Rate capability; 3) Cycling performance; 4) Safety; 5) Cost. The energy density is determined by the material's reversible capacity and operating voltage, which are mostly

determined by the material intrinsic chemistry such as the effective redox couples and maximum lithium concentration in active materials. For rate capability and cycling performances, electronic and ionic mobilities are key determining factors, though particle morphologies are also important factors due to the anisotropic nature of the structures and are even playing a crucial role in some cases. Figure 1.2 compared the gravimetric energy densities of different cathode materials that are currently under investigations. While some materials such as LiFeBO_3 and LiFeSO_4F are already approaching their theoretical energy densities, for other materials including conventional layered and spinel compounds, significant gaps are still present between their theoretical and practical energy densities. These materials with promising theoretical properties have high potentials as the candidates of future generation LIB cathode; however, their rate capacity and cycling performances still need much improvement before they can be commercialized.

1.2 High-energy high-power cathode material in Li-ion batteries

From the first commercialized cathode material LiCoO_2 to the current one of the best candidate for EV applications, Li-excess materials, they all adopted a layered structure. The ideal structure of layered compound LiMO_2 is demonstrated in Figure 3. The oxygen anions (omitted for clarity in the figures) form a close-packed fcc lattice with cations located in the 6-coordinated octahedral crystal site. The MO_2 slabs and Li layers are stacked alternatively. Although the conventional layered oxide LiCoO_2 has been commercialized as the LIB cathode for twenty years, it can only deliver about 140mAh/g capacity, which is half of its theoretical capacity. Such limitation can be attributed to the

intrinsic structural instability of the material when more than half of the Li ions are extracted. On the other hand, the presence of toxic and expensive Co ions in LiCoO_2 has introduced the environmental problem as well as raised the cost of the LIB.

For improvement, Co ions in LiCoO_2 can be substituted by other transition metal ions such as Ni and Mn. The new substitutions can reduce the cost of the materials and make the materials more environmentally friendly by eliminating the use of Co ions, which are expensive and toxic. One of the most promising candidates is so-called Li-excess nickel manganese layer oxides $\text{Li}[\text{Ni}_x\text{Li}_{1/3-2x/3}\text{Mn}_{2/3-x/3}]\text{O}_2$. The compounds were first reported in 2001 and can be expressed as a composite of two end members of $\text{Li}[\text{Li}_{1/3}\text{Mn}_{2/3}]\text{O}_2$ and $\text{LiNi}_{1/2}\text{Mn}_{1/2}\text{O}_2$. A reversible capacity as high as 250mAh/g can be obtained routinely.

1.3 Surfaces and Interfaces

Upon electrochemical cycling, significant variations in structures and chemical distributions occur, including ion relocation, lattice expansion/contraction, phase transition, and structure/surface reconstruction, etc. These variations could impose significant influence on ion/electron transportations, and thus the performance and lifetime of the whole system. In addition, the electrode consists of the active material, a good electronic conductor (graphite usually) and a binder. The interfaces in the active material and in between all the components are essential and most of the time limiting step of the ion/electron transportations.

Moreover, during the electrochemical performances, irreversible reactions occur simultaneously with the reversible Li shuffle in between the electrodes. For example, the

formation of a solid electrolyte interface (SEI), resulting from the decomposition of electrolytes on the surface of electrodes, would affect the kinetics of the system.

Understanding surface and interface properties are essential for the system optimization.

1.4 Objectives and overview

The objective of this research project is to understand the surface and interface properties of electrode materials in alkali-ion batteries using a combination of first principles computational methods and experimental characterization techniques. The project can be divided into four parts:

Part 1: Study the surface electronic and chemical properties during nanosizing effect and the associated increased functional capabilities

Part 2: Study the surface and interface structural and chemical evolution during electrochemical cycling and mechanism associated

Part 3: Study the coating effect on the electrode materials

Part 4: Study a new system in Na ion batteries

Chapter 1, in part, is a reprint of the material "Recent Progress in Cathode Materials Research for Advanced Lithium Ion Batteries", as it appears in Materials Science and Engineering R, 73(5-6), 51-65, 2012. Bo Xu, Danna Qian, Ziyang Wang, Ying Shirley Meng, 2012. The dissertation author was the primary investigator and author of this paper.

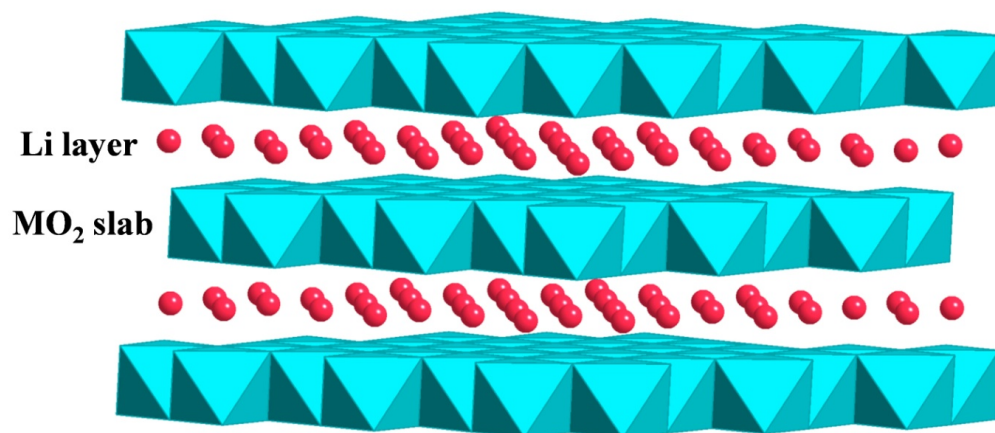
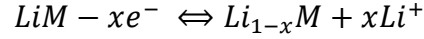


Figure 1.3: Crystal structure of layered LiMO_2 (Blue: transition metal ions; Red: Li ions)

2 FIRST PRINCIPLES METHOD AND ITS APPLICATION ON THERMODYNAMIC PROPERTIES OF INTERCALATION MATERIALS

2.1 Thermodynamics of intercalation materials

In intercalation material LiM, where M is the host structure and Li is the mobile ions, the following reaction happens during electrochemical charging/discharging:



The average voltage is therefore $V = \frac{\Delta G}{xze}$, where ΔG is the Gibbs free energy for the reaction, z is the valence of Li and e is the charge of the electron. Usually, the host structure M does not change during the charging/discharging process, therefore its chemical potential does not change. The electrochemical energy comes from the chemical potential difference of Li ions in both electrodes. The voltage therefore could be derived from the Nernst equation.

$$V(x) = -\frac{(\mu_{Li}^{cathode} - \mu_{Li}^{anode})}{ze}$$

Metal Li is always used as the counter electrode, μ_{Li}^{anode} is usually constant. From the knowledge of classical thermodynamics, the derivative of Gibbs free energy can be written as:

$$dG = Vdp - SdT + \sum \mu_i dN_i$$

Under the condition of constant pressure and temperature, the host structure does not change, therefore, the chemical potential of Li could be written as $\mu_{Li} = \left(\frac{\partial G}{\partial N_{Li}} \right)_{T,p,N_{host}}$, where N_{Li} is the number of lithium ions. The independent intensive variables of the system should be temperature T, pressure P, and the chemical potential μ . To investigate

the phase stability at different temperature or pressure, the characteristic potential should be grand canonical free energy rather than the Gibbs free energy. A Legendre transform is necessary that the grand canonical free energy

$$\Omega_{host} = G_{host} - N_{Li}\mu_{Li}$$

Since the host structure does not change, the number of host does not change. Therefore the formal transform can be rewritten as

$$\Omega_{host} = \frac{\Omega_{host}}{N_{host}} = \frac{G_{host} - N_{Li}\mu_{Li}}{N_{host}} = G_f^{host} = x\mu_{Li}$$

where x is regard as the Li concentration.

2.2 First principles energy calculations

2.2.1 General energy approximation

First principles theory is commonly used in the energy calculations. Also called as ab-initio, the theory starts directly at the level of the most basic physic laws, the atomic numbers and quantum mechanics. The Kohn-Sham energy function can be given that

$$E[\{\psi_i\}] = 2 \sum_i \psi_i \left[-\frac{\hbar^2}{2m} \right] \nabla^2 \psi_i d^3r + \int V_{ion}(r) n(r) d^3r + \frac{e^2}{2} \int \frac{n(r)n(r')}{|r-r'|} d^3r d^3r' \\ + E_{XC}[n(r)] + E_{ion}(\{R_I\})$$

where $n(r) = 2 \sum_i |\psi_i(r)|^2$ is the electronic density. On the right side of the equation, there are five terms that contribute to the total energy. The first item represents the electron kinetic energy from the original Schrödinger equation. The second term represents the electron-ion potential energy. The third term represents the electron-electron repulsion interactions. The forth term represents the exchange and correlations of

many-electron system beyond the direct coulomb repulsion. And the final term represents the coulomb interactions between different ions.

2.2.2 Density-functional theory

The density-functional theory (DFT) associates all the interactions to a uniform variable, the electronic charge density. The solution of the energy equation is obtained in a self-consistent way to ensure the accuracy. Since only the minimum of the solutions of the energy equation makes sense when investigate the ground state energy, the final term in above equation could be removed. Kohn-Sham equations therefore can be further simplified to

$$\left[-\frac{\hbar^2}{2m} \nabla^2 + V_{ion}(r) + V_H(r) + V_{XC}(r) \right] \psi_i(r) = \varepsilon_i \psi_i(r)$$

where $\psi_i(r)$ is the wave function of electronic state i . V_H is the Hartree potential of the electrons representing the electron-electron repulsion and V_{XC} is the exchange-correlation potential. All the potentials are equations related to the electronic charge density. Using self-consistent method, as long as the electronic charge density is obtained, the total energy could be calculated.

2.2.3 Generalized gradient approximation (GGA)

The major problem with DFT is that the exact functional for exchange and correlation are not known except for free electron gas. However, approximations exist which permit the calculation of certain physical quantities more accurately. The GGA, developed by Perdew and Yue, takes into account for the gradient of the density at the

same coordinate compared with local-density approximation (LDA). GGA has been proved to be more suitable in systems where the electronic states are highly localized in space, such as alkali transition metal oxides, most commonly used electrode materials. Moreover, in transition metal ions, the highly localized d electrons could cause the main error of the calculation accuracy because of the lack of cancellation of electron self-interaction. GGA + U method therefore is developed to circumvent this problem and is proved to be successful in Li intercalation materials.

2.2.4 Pseudopotential approximation

Besides the electron-electron interaction, the electron-ion interactions are also difficult to deal with because of the huge number of core-electrons of each ion. Since the core-electrons are tightly bonding with the nuclei, a large number of wave functions are needed for the fourier transformation, which will highly raise the cost of computation. It is necessary to do the full electron calculation if dealing with the fine electronic structure of the materials. However, most of the time, the major physical properties of the materials are determined by the valence electrons, which is usually no more than eight. The pseudopotential approximation is developed so that all the core-electrons are simplified as a core and the ion is divided into two parts, the “core” and the valence electrons. A local pseudopotential is set up that it will be exactly the same with the core electron potential beyond a critical distance r_c from the nuclei.

On one hand, the consistence between pseudopotential and full-electron potential beyond r_c ensures the correction of the properties that determined only by the valence electrons. On the other hand, the complicated core-electrons are substituted by only one

potential function therefore the computation cost is highly reduced. Again, since the pseudopotential of each element is only determined by the atomic number of the element, it could also be determined in a self-consistent way.

2.3 Surface and interface energy calculations

According to Tasker's definition, ionic crystals can be classified into three types. Type 1 is neutral with equal numbers of anions and cations on each plane and type 2 is charged but there is no dipole moment perpendicular to the surface because of the symmetrical stacking sequence. Both the two surfaces should have modest surface energies and may be stable with only limited relaxations of the ions in the surface region. Type 3 surface is charged and has a dipole moment in the repeat unit perpendicular to the surface. The surface can only be stabilized by substantial reconstruction. The three different types of surfaces are shown in Figure 2.1.

Type 1 and 2 are called non-polar surface and type 3 is called polar surface. For the first two types of surfaces, the calculation of surface energy is pretty straightforward, while for the third type, the energy would diverge and the surface energy is becoming infinite as the electrostatic interactions between unit cells are pretty large. As a result, if we want to get accurate results for the third type surfaces, surface modifications are needed. However, one thing to point out is that this surface may exist in nanostructures. Possible methods of the modifications are adsorption or desorption, reconstruction accompanied by surface vacancy creation.

The standard for calculating the surface is to evaluate the total energy of a slab of the material of interest and to subtract from that the bulk energy obtained from a separate calculation. It is based on the general and intuitively appealing expression:

$$\sigma = \lim_{n \rightarrow \infty} \frac{1}{2} (E_{slab}^N - NE_{bulk})$$

where E_{slab}^N is the total energy of the slab and E_{bulk} is the bulk total energy, $\frac{1}{2}$ term accounts for the two surfaces of the slab.

The reason for this equation is as follows. As plotted in Figure 2.2, Regions 1 and 3 are set wide enough so that the influence of the surface is negligible in region 2. In other words, the influence of the surface should vanish exponentially by increasing the widths of regions 1 and 3 when looking at orbitals at the surface and Wannier functions. This viewpoint suggests that with thick enough “surface regions” (regions 1 and 3) the “surface energy” should be defined regardless of the thickness of the region at the center (region 2) because the surface orbitals have negligible effect in region 2. The term “surface energy” will be used in this sense (surface energy in the infinitely thick slab limit) onwards.

Handling interface between two materials is similar to handling the surface of one material with vacuum. However, there are still many unsolved problem in this study.

The most straightforward methodology derived from the one surface calculation is that the interface energy can be extracted from the slab total energy minus the bulk energy of both materials. Complications arise on this point. First, for the interface buildup, two materials usually have different lattice parameters, while in nature, the interface is always perfectly formed, no strain. What is the most appropriate lattice parameter to use?

Secondly, the interface may be vague between two materials, what is the most appropriate bulk energy to use?

If we choose A's lattice parameter, B would be strained, and vice versa. If we choose the lattice parameter between A's and B's, both materials would be strained, and the effect is unknown comparing to one strained, one not. One other thing is that the strain contribution from the two materials is not known. This remains a big problem in the interface calculations.

Figures:

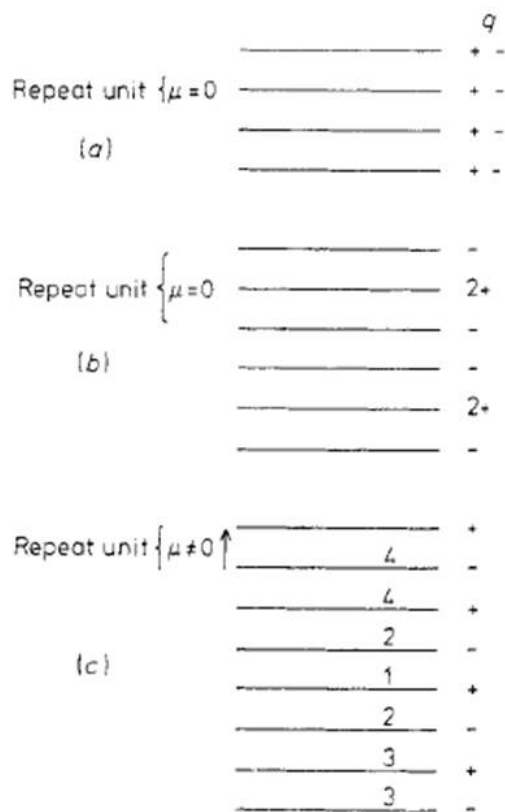


Figure 2.1: Three types of Tasker ionic crystal surfaces

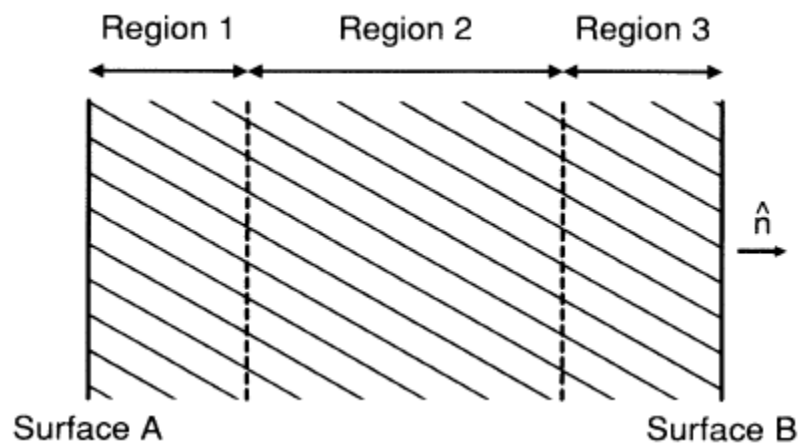


Figure 2.2: Schematic plot of surface and bulk

3. Advanced Analytical Electron Microscopy for Alkali-Ion Batteries

3.1 Introduction

In order to realize the commercialization of alkali-ion batteries (AIB) in electric vehicles and smart grid systems, further improvements are demanded in multiple aspects, especially the energy/power density, safety and cycle life. The performance of the batteries depend on the storage and diffusion of alkali-metal ions, electron transportation, structure and chemistry dynamics of the electrode/electrolyte materials, etc.. During electrochemical cycling, changes in structures and chemical distributions occur, including ion relocation, lattice expansion/contraction, phase transition, and structure/surface reconstruction, etc. These variations could impose significant influence on ion/electron transportations, and thus the performance and lifetime of the whole system. Understanding the structure-properties relationship of each component and their nanoscale evolution in the electrochemical process is essential for the design of new materials and optimization of existing systems.

The characterization of structure and electronic properties of each component is essential to understand and optimize battery materials. Multiple techniques have been developed both in-situ and ex-situ for structural and chemical characterizations, such as X-ray Diffraction, X-ray Absorption Spectroscopy, Neutron Diffraction, Nuclear Magnetic Resonance, etc.. However, only spatially averaged or surface-dominated information can be obtained from these techniques. On the other hand, structural and chemical evolutions upon electrochemical cycling often behave significantly different at nanofeatures, such as structural defects, boundaries, surfaces and interfaces, from that in

material bulk. Their influences on the functionalities of macroscopic devices are further magnified by the continuous device minimizations. Transmission electron microscopy (TEM), especially with the recently developed techniques such as aberration correctors and fast imaging cameras, has become one of the best techniques to probe these parameters at micron to atomic scale, under both static and in-situ electrochemical operations.

In this review article, firstly we will introduce the recent developments on TEM techniques that have been involved in or will be potentially valuable for the research of alkali-ion batteries. Then we will focus on the implementations of TEM in battery research by providing representative examples on how advanced microscopy significantly promotes our fundamental understanding of battery system and battery materials. Both advanced high-resolution electron microscopy and newly developed dynamic / in-situ TEM techniques for battery research will be reviewed. Last but not the least, perspectives regarding the future directions will be provided.

3.2 New progress on TEM

Over the past two decades, a number of significant improvements in TEM have provided substantial opportunities for fundamental new understanding of the working mechanisms in battery materials and systems, especially through the direct observations of atomic position and chemical bonds, as well as ion electron distributions at the atomic scale, Figure 3.1.¹⁻⁴ Aberration correction in TEMs has made it feasible to image and identify individual atoms. Single atomic columns can be routinely imaged.⁵⁻⁸ In particular, taking advantage of the various scattering processes that occur between the incoming

electrons and atoms in materials, analytical imaging techniques with various sensitivities can be simultaneously applied using multiple annular detectors in scanning transmission electron microscopy (STEM). A high angle annular dark field (HAADF) image provides an image contrast proportional to atomic number ($\sim Z^{1.7}$); while a smaller annular angle detector (Annular bright field ABF) gives a contrast of $\sim Z^{-1/3}$ that is ideal for the detection of light elements, such as lithium.^{9,10} A bright-field detector in STEM, which collects the elastically scattered electrons, provides phase contrast images equivalent to standard bright-field TEM images.¹¹ Low-angle annular dark-field imaging (LAADF), on the other hand, forms images by collecting both elastically and inelastically scattered electrons, providing opportunities for mapping strain fields in materials at atomic resolution.¹² Electron energy-loss spectroscopy allows probing electronic structures while collecting elastically scattered electrons only, and provides a complementary imaging mode with the unprecedented benefits of quantitatively probing both the chemistry and structure of nanofeatures at sub-Å resolution.^{6,13} With the recent development of monochromators for the electron gun, the energy resolution of EELS can now achieve 10meV, enabling not only the detections of electronic structure and atomic bonds, but also the investigations of vibration features in solid materials.^{1,14}

Alongside with these developments of ultra-high spatial and energy resolutions, remarkable advances have been made in developing new *in situ* techniques and platforms for TEMs. These techniques have enabled direct observations of dynamic structural and chemical evolution in materials under a variety of external stimuli or near-real operation conditions. The progress is evident and has been demonstrated especially in the advances of *in situ* mechanical testing or heating while maintaining a high spatial resolution,^{15,16} in

the studies of imaging reaction processes in gases and liquids,¹⁷⁻²⁰ and in the observations of reactions or phase transformations upon external biasing^{21,22}, etc. Along with the progress of *in situ* capabilities, the newly developed CMOS camera enables fast image acquisition of over 400 frame-per-second (FPS) for 1Kx1K images, and is significantly advancing real time observations of fast reactions.²³ These modern noteworthy advances in electron microscopy have opened broad opportunities for unraveling the mysteries in various materials and devices, and pinpointing the development and design of novel materials at the atomic scale.

3.3 HIGH RESOLUTION ELECTRON MICROSCOPY FOR BATTERY MATERIALS

Owing to the significantly enhanced spatial and energy resolutions, the state-of-art electron microscopy, including both atomic scale imaging and chemical analysis, has been applied extensively for probing the structural and chemical information of electrode and electrolyte materials as well as their interfaces in battery systems. These investigations have provided unique quantitative structure and chemical information benefiting both materials design and performance improvements in battery research.

3.3.1 Electrodes

Generally speaking, the electrode material can be divided into three types: intercalation, conversion and alloying materials. Intercalation based materials, which are the most commonly used in everyday batteries, are mainly transition metal oxides. The host structure does not change during the insertion and extraction of alkali-metal ions.

Conversion materials are mostly transition metal oxides and fluorides. The host structure would change upon cycling, and usually nanosized transition metal particles and lithium oxides would form after charging. For alloying type materials, the host and alkali metal would form alloy upon cycling, accompanied by volume change. TEM has played a crucial part in advancing the understanding of all three types of electrode materials. Two main aspects have been focused on using static TEM: structure identification and mechanistic study on the performance degradation mechanism. This part of the review will focus on how TEM helps and advances the development of representative compounds in the three categories.

3.3.1.1 Intercalation materials

The intercalation materials are of great interest in the history of cathode material development. Li-excess layered compounds, high voltage spinel, and olivine are the ones receiving the most attention due to their potential application in high-energy high-power electric vehicle. Even though the host structure remains the same during electrochemical process, Li concentration changes are always accompanied by diverse structural changes, such as lattice parameter variation, phase transition, surface reconstruction, etc. Electron microscopy provides a unique perspective on those processes down to the atomic level.

The family of Li-excess layered materials, $x\text{Li}_2\text{MnO}_3 \square (1-x)\text{LiMO}_2$ (M=Mn, Ni, Co, Fe, Cr, etc.), despite their good performances and the increasing attention they received, present many challenges for understanding the pristine-state structure and reaction mechanism that deteriorate the performances. Regarding the structure, there is a long-standing debate on whether it is a solid solution or two separate phases composing of R-

3m and C2/m. X-ray and neutron diffraction cannot give the exact information due to the overlap in peaks as well as the domain structure associated. This difficulty can be overcome by electron microscopy. Jarvis et al. discovered a solid solution in their Li-excess layered material²⁴ and identified planar defects formed from disordered R-3m to C2/m state.²⁵ Bareno et al. found a locally Li_2MnO_3 -like region in the parent rhombohedral structure.²⁶ Boulineau observed the coexistence of two phases with the nominal composition.²⁷ Because of the atomic configurations unraveled by the STEM/EELS studies, it has now been agreed that the transition metal species, stoichiometry, synthesis methods, and calcination temperatures are important factors determining the structures.

The first-cycle irreversible capacity and the voltage degradation upon cycling are the main obstacles to the final commercialization. Therefore, understanding the reaction mechanism especially the first cycle is critical. Different proposals have been made including the activation of oxygen, the surface phase transformation to spinel-like/rocksalt structure, surface TM densification, etc.. Meng group carried out a series of systematic studies starting from electron microscopy.²⁸⁻³¹ A surface layer of defect spinel has been visualized for the first time and also been confirmed by many following studies.^{27,32} The presence of the transition metal (TM) ions in the lithium layer has been evidenced by Z-contrast imaging, and the formation of defect spinel phase has been confirmed by EELS and first principles computation. By identifying the structural and chemical changes at different states of charge, a mechanism involving both bulk and surface is proposed. In addition, a novel oxygen-vacancy-assisted TM migration mechanism has been proposed to the surface phase transformation. (Summarized in

Figure 3.2) Later, Boulineau et al. proposed a densification model based on the observation of Ni/Mn segregation on the surface by STEM/EELS.³² Researchers from PNNL also carried out several studies on this family of material and revealed the influence of nonuniform TM distribution and nanophase separation on the electrochemical performance.³³

Li-excess family is a representative case of what electron microscopy can do in advancing scientists' understandings in battery materials. Clearly, many main pieces to solve the structure and mechanism puzzle can only be obtained by electron microscopy, such as the surface phase transformation, the chemical information along the interface, etc. By combining with other techniques, the mechanism is vividly presented.

Another good example is the investigation of atomic defects in olivine LiFePO_4 . LiFePO_4 has attracted the most interest among all polyanion materials in battery research, owing to its low cost, non-toxicity, excellent thermal stability and environment friendliness. However, its intrinsic atomic structural defects, originating from the site exchange between Li and Fe (denoted as Fe_{Li}), also called as "anti-site defects", are the main structural characteristic limiting the electrochemical performance. Due to the one-dimensional Li^+ transport in LFP, such defects could significantly degrade the performance from two aspects: blocking the ion transportation and restraining the amount of available Li. Detecting the concentration and distribution of Fe_{Li} in this material thus is crucial to the performance improvement. Due to the small atomic number of Li, neutron diffraction was able to quantify the defects. The exact distribution of defects, however, remained unknown until the application of ADF imaging in electron microscope. Chung et al. discovered a locally aggregation behavior of Fe_{Li} through imaging and image

simulations.^{34,35} Later on, a vacancy driven mechanism for such local segregation was proposed based electron microscopy results, depicted in Figure 3.3(a).³⁶

In addition to defects quantification, the direct identification of reaction mechanisms in LFP during electrochemical process is another significant contribution of advanced electron microscopy to LFP research. It has been macroscopically identified that two-phase, i.e. $\text{LiFePO}_4\text{-FePO}_4$ are involved in during cycling, and such reaction however was supposedly limiting the reaction dynamics. To the opposite, it shows an unexpected excellent rate capability for long-term cycling. Attention was thus attracted to the cycling mechanism at the phase boundaries. Thanks to TEM, it was possible to directly probe the phase boundary at the atomic level. Multiple novel microscopy techniques were combined to investigate such phase boundaries, including HRTEM, electron diffraction, EELS, and precession electron diffraction etc..³⁷⁻⁴⁰ Several working mechanism at $\text{LiFePO}_4\text{-FePO}_4$ phase boundaries, including core-shell,³⁸ spinodal³⁹ and domino cascade⁴⁰ were proposed based on microscopy results, consistent with the development of models from other techniques. Though no consensus has been achieved at current stage, these studies have provided invaluable information towards the understanding of working mechanism in 1-D diffusion battery materials.

These recent microscopy studies on intercalation materials discussed above well demonstrated the power of novel electron microscopy of its atomic-scale detectability of structure, chemistry, as well as bonding information for battery research.

3.3.1.2 Conversion and Alloying materials

Conversion materials, designed to utilize all possible oxidation states of transition metal, suffer from poor cycling retention and large hysteresis. Due to the formation of nano-sized particles after cycling, HAADF-STEM can be used to visualize the phase conversion due to the large difference between the contrast from metallic particles and that from lithium oxides/fluorides. Besides the image contrast, the elemental mapping can also provide the phase information at atomic resolution. Fluorides and oxyfluorides are attracting the attention due to their potential to serve as cathode materials with capacities up to 600mAh/g. Iron fluorides exhibit a superior cycling performance compared with other metal fluorides, for example, the reversibility of FeF_2 is much higher compared with CuF_2 while the reason was unclear. Owing to the ability of simultaneous morphology probing and elemental identification at high-spatial resolution in STEM, Wang et. al. discovered a conductive iron network formed for FeF_2 after cycling while discrete particles in the CuF_2 case by combining HAADF imaging and EELS analysis, shown in Figure 3.3 (c) & (d). This work reveals that the low electron conductivity is the source of poor reversibility in CuF_2 .⁴¹ Besides, several other research groups have used similar microscopy techniques and identified the conversion mechanisms of iron fluorides and iron oxyfluorides.^{42,43}

The most representative alloying materials for battery electrodes is Si-based. These materials are considered as a strong candidate as negative electrodes, owing to an exceptional capacity of ~ 4200 mAh/g, compared to the 372mAh/g of the commercially used graphite. The practical use of silicon is, however, hindered by a massive 280% volume expansion during the charge–discharge process. Such a drastic change leads to loss of electric connections in the electrode.⁴⁴ It is therefore of special importance to

understand the exact chemical reactions and possible crystalline-to-amorphous transitions happening during cycling. Microscopy is an ideal tool for such studies as it provides high sensitivity not only to crystalline phases, but also amorphous ones. Using EELS, imaging and diffraction techniques, not only the final reaction products but intermediate phases of Li_xSi have been identified, providing valuable insights into structural and morphology optimizations of Si-based material for battery applications.^{45,46} In addition, direct observations of the volume change and phase transformations in Si-based materials have been demonstrated because of the new developments of in-situ TEM techniques, which will be discussed latter in this article.

These studies demonstrated high resolution AEM provides unique insights into the atomic scale structural/chemical origin of the macroscopic behaviors during cycling. Although having limitations under certain circumstances, the TEM observation has played a vital role in understanding the electrochemical process of multiple extensively studied electrode materials.

3.3.2 Electrolyte

Due to the safety concerns associated with the flammability and leakage of conventional liquid electrolyte, the stable solid electrolytes have received tremendous attention.⁴⁷ However, the study of solid electrolytes using TEM is challenging: because of the vanishingly small electronic conductivity, the radiation damage is much more severe than that for the cathode materials.^{41,48,49} As a result, the atomic-resolution TEM studies on solid electrolytes are rare.^{46,49-56} Regardless, most of these papers provided unique insights into the ionic conduction behaviors, and laid important groundwork for the

design and discovery of high-performance solid electrolytes. The primary bottleneck for the application of solid electrolytes is the low conductivity. A rational improvement strategy cannot form without a proper understanding on the Li^+ transport behaviors. The perception of this phenomenon consists of three aspects: the Li^+ transport 1) within the lattice, 2) along/across the grain boundaries, and 3) across the electrode/electrolyte interfaces. While the study of the first one frequently benefits from quite a lot of characterization techniques, the other two, in many cases, can only be straightforwardly studied by TEM.

The Li^+ conduction behavior within the lattice is dictated by the Li^+ percolation pathways. As such, the crystal structure and Li distribution are consistently the focal point in literature. The high spatial resolution and sensitivity to minor structure differences make TEM particularly suitable for such a task. Using precession electron diffraction, which has the advantage of minimizing the distraction from double diffractions, Buschmann *et. al.* successfully distinguished between the tetragonal and cubic phases of the garnet $\text{Li}_7\text{La}_3\text{Zr}_2\text{O}_{12}$.⁴⁹ The disordered Li distribution in the cubic polymorph with respect to the tetragonal one is essential in explaining the high ionic conductivity of the former. In the same paper, efforts have also been made to study the atomic structure via HRTEM, but only limited information was acquired due to the quick amorphization of the material under electron beam. Recently, this difficulty was overcome by Ma *et. al.*⁵⁶ By weakening the electron beam current and using a cryogenic stage, the atomic structure of HAADF-STEM was finally visualized. In addition to the crystal structure, TEM is also very effective in probing the local Li distribution. Gao *et. al.* has took full advantage of the imaging capability of ABF and precisely determined the

Li position in $(\text{Li}_{3x}\text{La}_{2/3-x})\text{TiO}_3$,⁴⁶ a system showing the highest bulk conductivity among all the oxide solid electrolytes, shown in Figure 3.4 (a-b).⁴⁷ Furthermore, the Li content, valence state of Ti, and geometry variation of oxygen octahedra in the alternating La-rich and La-poor layers were revealed via the associated EELS analysis.⁴⁷ The Li migration pathway was delineated based on these observations. Beyond this, the same authors reported the local structure/chemistry variation across the boundaries between the La-rich/poor ordering domain, and concluded that the domain boundaries serve as obstacles for the Li transport.⁵¹ The precise analysis of such local features brings invaluable insights in interpreting the ionic conduction mechanism.

Although most studies on solid electrolytes focus on the Li migration within the lattice, the grain boundaries are no less important. The bulk conductivity of many solid electrolytes is actually sufficiently high for application.⁴⁷ It is their large grain-boundary resistance that lowers the total conductivity by orders of magnitude.⁴⁷ Unfortunately, due to the ignorance of the grain-boundary conduction mechanism, no effective improvement strategy has formed. Since the grain boundaries are typically as thin as several unit cells, the ultrahigh spatial resolution in TEM is an ideal tool to study them. Recently Ma *et. al.* has made the first attempt of scrutinizing the structure and chemistry of grain boundaries in $(\text{Li}_{3x}\text{La}_{2/3-x})\text{TiO}_3$, a typical example of a Li^+ superionic conductor being plagued by the poor grain-boundary conductivity, details in Figure 3.4 (c-e).⁵⁵ A local structural fluctuation was found to prohibit the abundance of Li, and thus hinders the ionic transport. The capability of TEM in resolving such issues is clearly demonstrated. Nevertheless, currently not much effort has been devoted towards this direction, and the grain-boundary conduction mechanism for many important systems remains unknown.

Finally, TEM is also very effective in studying the interfaces. Similar to the solid-electrolyte-interphase (SEI) layer in conventional Li-ion batteries with organic liquid electrolyte, interface layers were frequently observed between the intercalation cathodes and solid electrolytes.⁵²⁻⁵⁴ A fundamental understanding of the structure and chemistry of the interfaces is indispensable in optimizing the battery performances. Based on the combined imaging and EDX analyses, the interface in most systems was found to form via the mutual diffusion between the cathode and solid electrolyte.⁵²⁻⁵⁴ Unlike the SEI layers in the conventional Li-ion batteries, such interfaces are more detrimental than beneficial; their existence typically introduces a large interfacial resistance and degrades the battery performance.⁵²⁻⁵⁴

In summary, TEM is a very effective tool in studying the ionic transport mechanism of solid electrolytes. Its high spatial resolution offers unique convenience in studying localized features such as grain boundaries and interfaces. However, since the electron radiation damage is especially difficult to control for the solid electrolyte, currently the atomic-resolution STEM/EELS studies can only be performed in a very limited number of systems. Clearly, the implementation of such a powerful tool in the study of solid electrolytes demands a comprehensive investigation of the radiation damage mechanism that can guide the optimization of electron beam condition for each specific system.

3.4 DYNAMIC/IN-SITU MICROSCOPY FOR BATTERY RESEARCH

Due to the dynamic nature of the electrochemical process, it is important to reveal the real-time structural/chemical variations in battery materials to completely understand

the working or degradation mechanisms involved in, which however, is often beyond the ability of ex-situ characterizations. As a result, many in-situ techniques based on either spectroscopy or imaging, e.g. X-ray diffraction, Raman spectroscopy, Nuclear Magnetic Resonance, Scanning Electron Microscopy, etc., have been developed for this purpose. Among the different in-situ techniques, in-situ TEM, which possesses the unique capability of directly visualizing the materials behavior in real time with a high spatial resolution, naturally received intensive attention. However, in-situ electrochemical cycling in the high vacuum chamber of TEMs is challenging, mainly because (1) a limited size of a electrochemical cell can be investigated because of narrow pole-piece gap in microscope and the pre-request of sample thickness -- beam transparent; and (2) the cell design has to be high-vacuum friendly. The first limitation arises challenges to specimen preparation, material selection and biasing control etc., and the second one challenges the use of organic electrolytes which is the most common one being used in battery labs. In the following sections, we will discuss the details of the leading three in-situ microscopy configurations in battery research.

3.4.1 Open-cell configuration

In an open-cell configuration, as shown in Figure 3.5(a), the electrolyte is either solid Li_2O or an ionic liquid, which makes point contacts with the electrode. The low vapor pressure of ionic liquid makes it possible to be directly loaded and observed inside a TEM vacuum chamber. An overpotential is then applied and Li is driving from one electrode to the other. The lithiation process of several electrode materials is studied by this configuration. Intensive work from this type of set-up focuses on the alloying type

anode because the large volume change can be readily detectable using such simplified configuration. Liu and his colleagues reported for the first time the direct observation of anisotropic swelling of Si nanowires during lithiation.⁵⁷ Their following studies further revealed electrochemical process on nanostructured Si with different sizes.⁵⁸ Later on, the observation of such lithiation process at atomic-scale was achieved, enabling the discovery of a layer-by-layer peeling mechanism of the lithiation process on Si {111} facets.⁵⁹ Such mechanisms seamlessly explain the orientation-dependent Li mobility in Si. Using the same configuration, several other in-situ studies have been reported on multiple types of materials. Wang et. al. studied the lithiation mechanism of amorphous SnO₂ nanowires and observed a simultaneous partitioning and coarsening characteristics of Li_xSn through Sn and Li diffusion.⁶⁰ Zhu et al. imaged the FP/LFP phase boundary movement during electrochemical cycling for the first time.⁶¹ In addition, the conversion reaction for FeF₂ was observed to start at the surface and propagates into the bulk similar to a spinodal decomposition by using the same half-cell point-contact configuration.⁶² As such half-cell configuration uses Li metal as counter electrode and limits material choices in experiments, full-cell set-ups have also been tried. Huang applied LiCoO₂ as counter electrode to SnO₂ and observed a reaction front propagating in SnO₂ nanowire, depicted in Figure 3.5(b).⁶³

In-situ open cell set-up in TEMs has provided invaluable nano-scale information for fundamental understandings of reaction mechanism in various electrode materials. However, its intrinsic simplified configuration not only limits the selection of materials, especially the selection of electrolytes, but also the potential of recording corresponding electrochemistry data. Furthermore, controlled reversibility, i.e. precise lithiation and

delithiation, based on such configuration is also tricky. Other in-situ configurations thus have been developed accordingly.

3.4.2 Liquid-cell configuration

The aforementioned limitations of the open-cell setup stimulated the development of other configurations that can better mimic the actual batteries. One promising strategy is the liquid-cell configuration, where a fully functioning miniature battery is sealed with silicon nitride membranes to avoid the evaporation of the liquid electrolyte. In contrast to the open-cell setup, the liquid-cell configuration not only allows for the integration of the commonly used electrolyte, but also preserves the way that the electrode is in contact with the electrolyte as in real batteries. With such advantages, valuable insights that are difficult to obtain in the open-cell configuration were acquired. When Gu et al. applied the liquid-cell configuration for battery study (Figure 3.6(a)), they not only observed the lithiation/delithiation process of single Si nanowires that are consistent with the open-cell studies, but also successfully unraveled the dynamics of the electrolyte, which is difficult to probe using the open-cell setup. This result could entail a new and effective quantitative characterization for the formation of the solid-electrolyte interphase (SEI) layer.⁶⁴ Following this pioneering work, Zeng et al. observed Li metal dendritic growth as well as the SEI layer formation (Figure 3.6(b-c)).²³ In addition, Holtz et al. also used a similar configuration to determine the lithiation state of LiFePO_4 in real time with a relatively high spatial resolution.⁶⁵

Despite these valuable discoveries, the liquid-cell configuration has limitations. One of its most important drawbacks is the low spatial resolution. The presence of silicon

nitride membranes and the liquid electrolyte reduces the electron transparency of the miniature battery and undermines the spatial resolution. As a result, the liquid cell configuration is only suitable for probing the morphology change, *e.g.* Li dendrite growth, but cannot straightforwardly study the detailed structure/chemistry evolution at the atomic scale. Unfortunately, the latter is frequently more essential in perceiving the electrode processes. Clearly, preserving the full functions in miniature batteries is not sufficient for a detailed *in-situ* TEM study; minimizing/eliminating the additional thickness and maintaining the high spatial resolution are of no less importance.

3.4.3 All-solid-state micro-battery

The all-solid-state micro-battery approach can well circumvent the shortcomings of the liquid cell without sacrificing the integrity of the batteries. In this configuration, the Focused Ion Beam (FIB) is used to fabricate a cross-sectional lamella out of an all-solid-state thin film battery, as shown in Figure 3.6 (d). Such a lamella not only preserves the full functions of the thin-film battery, but also thin enough (≤ 100 nm) for electron transparency. Without the interference from the silicon nitride membranes and organic electrolytes in the liquid cell configuration, the all-solid-state micro-battery approach can provide much more detailed structural and chemical information in a much higher spatial resolution. In 2010, Yamamoto *et. al.* successfully applied this configuration to visualize the electric potential variation during the charge/discharge processes for the first time.⁶⁶ Using a piece of 90 μm thick NASICON-type glass ceramic (Ohara Inc.) as the electrolyte and 800nm thick LiCoO_2 as the cathode, the pristine-state battery is configured as $\text{Au}/\text{LiCoO}_2/\text{solid-electrolyte}/\text{Pt}$. During the first charge, a certain thickness

of the solid electrolyte near Pt was reduced, serving as the anode in the following discharge. With such setup, the 2D potential distribution resulting from movement of Li^+ near the LiCoO_2 /solid electrolyte interface was clearly visualized. Such a success stimulated an intensive interest in further perfecting the all-solid-state micro-battery approach for more in-depth analysis.

Despite its apparent advantages, presently this technique is much less developed than the other two discussed above; many problems remain to be addressed. First of all, the small thickness of the micro batteries (usually 100 nm or less) poses a formidable challenge. The successful cycling of a Li-ion battery usually demands a current density no larger than a few or tens of mA/cm^2 (otherwise the battery will fail catastrophically).⁶⁷ Because of the small dimension of the lamella for TEM observation, an extremely weak current of a few pA is required to meet this requirement. Realizing such a high current resolution is challenging for most *in-situ* TEM holders. Secondly, the stability of solid electrolytes also brings complications. Although not volatile like the liquid organic electrolytes, quite a few solid electrolytes are air- or moisture-sensitive. For example, the most important thin-film electrolyte, LiPON, can easily decompose by reacting with the moisture in air, and almost all sulfide solid electrolytes, despite their high conductivity, suffers severely from hydrolysis issues.⁴⁷ Therefore, appropriate air protection is needed for specimen transfer and storage. Thirdly, the re-deposition during the FIB fabrication of the micro-batteries could easily cover both the cathode and anode, shorting the entire battery stack. Last but not least, many solid electrolytes are subject to damage under intense electron beam in the (S)TEM. The imaging condition needs to be cautiously controlled to preserve the battery integrity during observation. Because of these

challenges (and possibly many other unknown difficulties), the full charge/discharge cycle has never been reported again after Yamamoto's *in-situ* electron holography study in 2010. Only several relatively successful attempts have been made. For example, Meng *et. al.* have tried to perform *in-situ* TEM studies on Au/SnO₂/Li_{3.4}V_{0.6}Si_{0.4}O₄/LiCoO₂/Pt⁶⁷ and Au/LiCoO₂/LiPON/Si/Cu⁶⁸ batteries. Although neither of them realized a full charge/discharge cycle, the element distribution across the interfaces was successfully visualized (Figure 3.6 (e,f)), and valuable experiences of fabricating a functioning micro-battery lamella were obtained. Clearly, the all-solid-state micro-battery configuration is still in its infancy stage compared to the open cell and liquid cell. However, it holds the greatest promise in unraveling atomic-scale structure/chemistry evolution during battery operation, and is thus attracting increasingly intense interest.

3.5. CONCLUSIONS AND PERSPECTIVES

In this review, we focus on the importance and recent progresses of (S)TEM study in alkali-ion batteries. With the remarkable development of the instruments, many of the previously formidable tasks, such as visualizing the distribution of light elements, unraveling the interface structure/chemistry at the atomic scale, and probing the SEI layers, *etc.*, have now become viable. Such capabilities greatly deepened the fundamental understanding of multiple important electrode and solid electrolyte materials. Beyond the static and *ex-situ* studies, various *in-situ* TEM techniques are also developed to study the dynamic electrochemical processes during charge/discharge. Among the three categories of the most extensively pursued *in-situ* TEM techniques, the all-solid-state micro-battery approach can well circumvent all the primary shortcomings of the open-cell and liquid-

cell configurations without compromising the battery integrity. These characteristics make it highly promising for realizing the atomic-scale observation of the real-time structure/chemistry evolution during battery operation, which is the key to comprehending and improving the battery performances. Therefore, although this technique is still in its infancy and poses many challenges, it is attracting increasingly intense research interests.

Chapter 3, in full, is a reprint of the material “Advanced analytical electron microscopy for alkali-ion batteries”, as currently being submitted for publication in *Asia Materials*. The dissertation author was the primary investigator and author of this paper. Most of the writing was conducted by the author.

Figures:

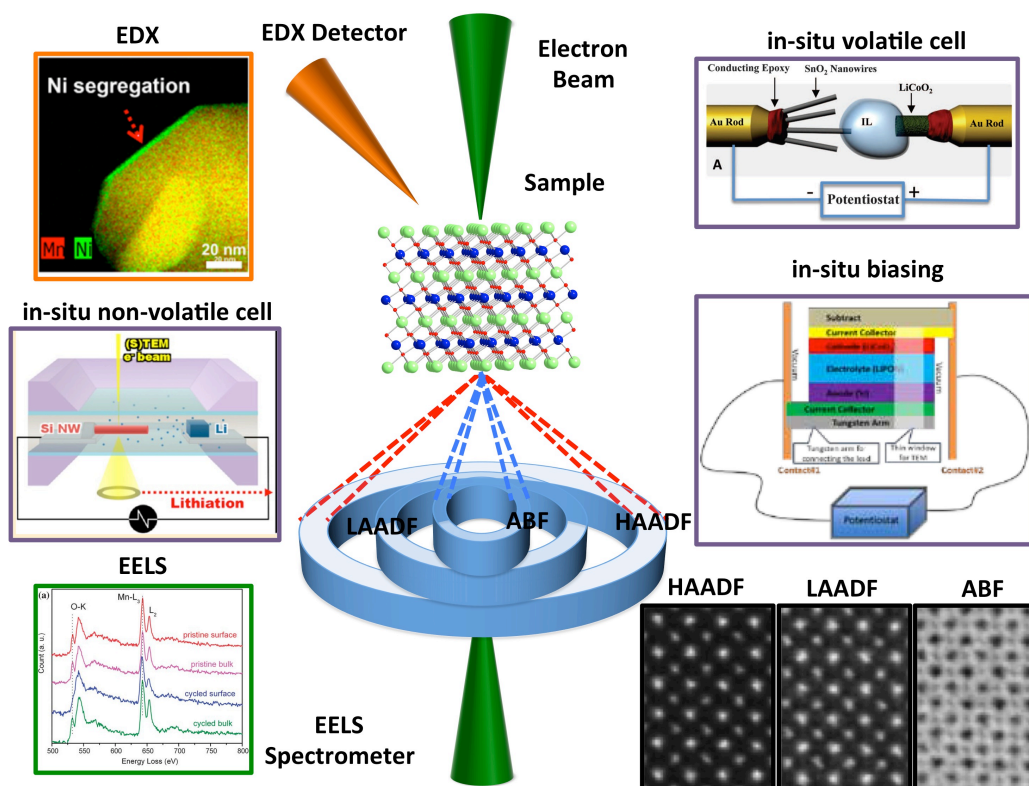


Figure 3.1: Overview of the implementation of TEM in AIB.

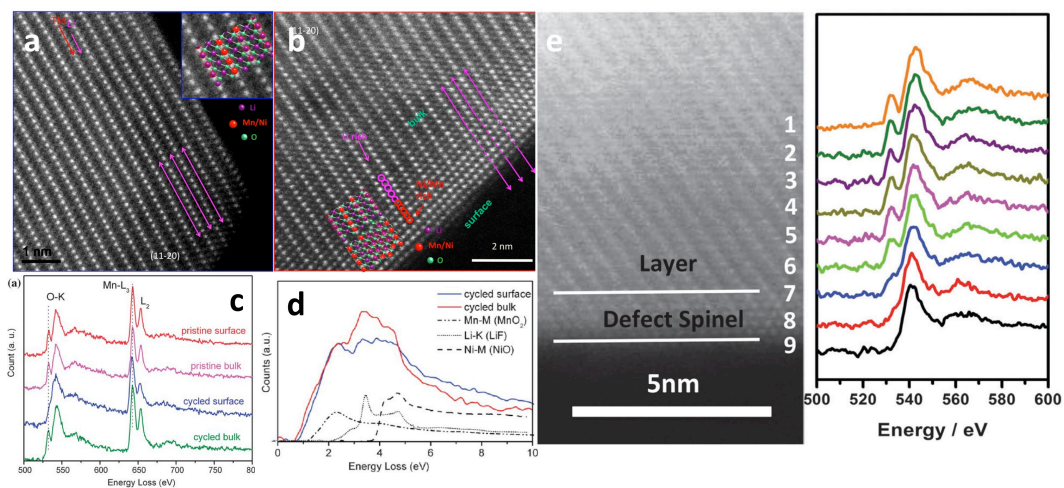


Figure 3.2: HAADF STEM images of Li-excess materials (a) pristine and (b) after cycling; (c) & (d) EELS comparison of pristine and cycled surface and bulk; (e) Spatial resolved O K-edge EELS from surface to bulk in cycled Li-excess.